CONFIDENTIAL

PERMANENT FILE COPY

# NACA

# RESEARCH MEMORANDUM

for the

Air Materiel Command, U. S. Air Force

INVESTIGATION OF STABILITY AND CONTROL CHARACTERISTICS

OF A $\frac{1}{10}$-SCALE MODEL OF A CANADIAN TAILLESS

GLIDER IN THE LANGLEY FREE-FLIGHT TUNNEL

By

Joseph L. Johnson

Langley Aeronautical Laboratory
Langley Air Force Base, Va.

# NATIONAL ADVISORY COMMITTEE
# FOR AERONAUTICS
## WASHINGTON

MAR 29 1949

CONFIDENTIAL

CONFIDENTIAL

# NATIONAL ADVISORY COMMITTEE FOR AERONAUTICS

## RESEARCH MEMORANDUM

for the

### Air Materiel Command, U. S. Air Force

## INVESTIGATION OF STABILITY AND CONTROL CHARACTERISTICS

## OF A $\frac{1}{10}$-SCALE MODEL OF A CANADIAN TAILLESS

## GLIDER IN THE LANGLEY FREE-FLIGHT TUNNEL

By Joseph L. Johnson

### SUMMARY

An investigation of the stability and control characteristics of a $\frac{1}{10}$-scale model of a Canadian tailless glider has been conducted in the Langley free-flight tunnel. The glider designated the N.R.L. tailless glider has a straight center section and outboard panels sweptback $43^\circ$ along the leading edge of the wing. The aspect ratio is 5.83 and the taper ratio is 0.323.

From the results of the investigation and on the basis of comparison with higher-scale static tests of the National Research Council of Canada, it is expected that the longitudinal stability of the airplane will be satisfactory with flap up but unsatisfactory near the stall with flap down. The airplane is expected to have unsatisfactory lateral stability and control characteristics in the design configuration with either flap up or flap down. The model flights showed very low damping of the lateral oscillation. Increasing the vertical-tail area improved the lateral stability, and it appeared that a value of the directional-stability parameter $C_{n_\beta}$ of at least 0.002 per degree would probably be necessary for satisfactory lateral flying characteristics. A comparison of the calculated dynamic lateral stability characteristics of the N.R.L. tailless glider with those of a conventional-type sweptback airplane having a similar wing plan form and about the same inclination of the principal longitudinal axis of inertia showed that the tailless glider had poorer lateral stability because of the relatively larger radius of gyration in roll and the smaller damping-in-yaw factor $C_{n_r}$.

### INTRODUCTION

An investigation of the low-speed stability and control characteristics of a $\frac{1}{10}$-scale model of a Canadian glider designated the N.R.L. tailless glider has been conducted in the Langley free-flight tunnel at the

request of the Air Materiel Command, U. S. Air Force. This tailless glider is based on a design of the National Research Council of Canada (NRCC) and has a wing with straight center section and outboard panels having $43^\circ$ sweepback of the leading edge. The outboard panels are equipped with trimming tips, which are adjustable for use in trimming the airplane. Vertical tails are located at the wing tip. The aspect ratio of the wing is 5.83 and the taper ratio is 0.323. The wing has a straight, center-section flap that hinges at the 0.70-percent center-section chord line and has a $60^\circ$ deflection.

The investigation included force and flight tests of the model in the flap-up and flap-down configurations to determine the longitudinal and lateral stability characteristics. Tests were made with increased vertical-tail area to determine whether the lateral stability and control characteristics of the model could be improved.

Calculations were made to determine the neutral-lateral-oscillatory stability and the period and damping data for the model in the flap-up and flap-down configurations with the design tail and with increased vertical-tail area.

## SYMBOLS AND COEFFICIENTS

$S$      wing area, square feet

$\bar{c}$      mean aerodynamic chord, feet

$b$      wing span, feet

$q$      dynamic pressure, pounds per square foot

$\rho$      air density, slugs per cubic foot

$m$      airplane mass, slugs

$\mu$      relative density factor $(m/\rho Sb)$

$\alpha$      angle of attack of reference axis (fig. 1), degrees

$\beta$      angle of sideslip, degrees

$\psi$      angle of yaw, degrees

$\eta$      angle of attack of principal longitudinal axis of airplane, positive when principal axis is above flight path at nose (fig. 1), degrees

$\epsilon$      angle between reference axis and principal axis, positive when reference axis is above principal axis at nose (fig. 1), degrees

$\theta$        angle between reference axis and horizontal axis, positive
when reference axis is above horizontal axis at nose
(fig. 1), degrees

$\gamma$        angle of flight to horizontal axis, positive in a climb
(fig. 1), degrees

R        Routh's discriminant ($R = BCD - AD^2 - B^2E$ where $A$, $B$, $C$, $D$,
and $E$ are constants representing coefficients of the
lateral-stability equation)

$k_{X_O}$        radius of gyration about principal longitudinal axis, feet

$k_{Z_O}$        radius of gyration about principal vertical axis, feet

$K_{X_O}$        nondimensional radius of gyration about principal longitudinal
axis $\left(k_{X_O}/b\right)$

$K_{Z_O}$        nondimensional radius of gyration about principal vertical
axis $\left(k_{Z_O}/b\right)$

$K_X$        nondimensional radius of gyration about longitudinal stability
axis $\left(\sqrt{K_{X_O}{}^2\cos^2\eta + K_{Z_O}{}^2\sin^2\eta}\right)$

$K_Z$        nondimensional radius of gyration about vertical stability
axis $\left(\sqrt{K_{Z_O}{}^2\cos^2\eta + K_{X_O}{}^2\sin^2\eta}\right)$

$K_{XZ}$        nondimensional product-of-inertia parameter
$$\left(\left(K_{Z_O}{}^2 - K_{X_O}{}^2\right)\cos\eta\,\sin\eta\right)$$

$C_L$        lift coefficient (Lift/qS)

$C_D$        drag coefficient (Drag/qS)

$C_m$        pitching-moment coefficient (Pitching moment/qS$\bar{c}$)

$C_n$        yawing-moment coefficient (Yawing moment/qSb)

$C_l$        rolling-moment coefficient (Rolling moment/qSb)

$C_Y$        lateral-force coefficient (Lateral force/qS)

$\delta_c$        controller deflection, degrees

$\delta_a$        aileron deflection, degrees

$\delta_f$         flap deflection, degrees

$C_{Y_\beta}$      rate of change of lateral-force coefficient with angle of sideslip, per degree $(\partial C_Y/\partial\beta)$

$C_{n_\beta}$      rate of change of yawing-moment coefficient with angle of sideslip, per degree $(\partial C_n/\partial\beta)$

$C_{l_\beta}$      rate of change of rolling-moment coefficient with angle of sideslip, per degree $(\partial C_l/\partial\beta)$

$C_{Y_p}$      rate of change of lateral-force coefficient with rolling-angular-velocity factor, per radian $\left(\partial C_Y \middle/ \partial\frac{pb}{2V}\right)$

$C_{l_p}$      rate of change of rolling-moment coefficient with rolling-angular-velocity factor, per radian $\left(\partial C_l \middle/ \partial\frac{pb}{2V}\right)$

$C_{n_p}$      rate of change of yawing-moment coefficient with rolling-angular-velocity factor, per radian $\left(\partial C_n \middle/ \partial\frac{pb}{2V}\right)$

$C_{l_r}$      rate of change of rolling-moment coefficient with yawing-angular-velocity factor, per radian $\left(\partial C_l \middle/ \partial\frac{rb}{2V}\right)$

$C_{Y_r}$      rate of change of lateral-force coefficient with yawing-angular-velocity factor, per radian $\left(\partial C_Y \middle/ \partial\frac{rb}{2V}\right)$

$l$      tail length (distance from center of gravity to rudder hinge line), feet

$\bar{z}$      height of center of pressure of vertical tail above fuselage axis, feet

$p$      rolling angular velocity, radians per second

$r$      yawing angular velocity, radians per second

$P$      period of oscillation, seconds

$T_{1/2}$      time for amplitude of oscillation to decrease to half amplitude

$T_2$      time for oscillation to double amplitude

$C_{1/2}$   cycles for amplitude of oscillation to decrease to half
     amplitude

$C_2$   cycles for oscillation to double amplitude

## APPARATUS

### Wind Tunnel

The investigation was made in the Langley free-flight tunnel which
is designed to test free-flying dynamic models. A complete description
of the tunnel and its operation is given in reference 1. The force tests
to determine the aerodynamic characteristics of the model were made on
the free-flight-tunnel six-component balance which is described in refer-
ence 2. The balance rotates in yaw with the model so that all forces
and moments are measured with respect to the stability axes. (See fig. 2.)

### Model

The $\frac{1}{10}$-scale model used in the investigation was constructed at the
Langley Laboratory. A three-view drawing of the model is presented in
figure 3 and photographs of the model are given in figures 4 and 5.
Table I gives the dimensional and mass characteristics of the full-scale
design and scaled-up dimensional and mass characteristics of the model.
The airfoil section used on the model was a modified Rhode St. Genese
35 airfoil section described in reference 3. The substitution of this
highly cambered airfoil section for that specified was in accordance
with free-flight-tunnel practice of using airfoils to obtain a maximum
lift coefficient in the low-scale tests more nearly equal to that of
the full-scale design than is possible with the design airfoil. The
trailing edge of the wing center section and the inboard portion of the
sweptback panels were provided with trimmers so that the large pitching
moment given by the cambered wing could be trimmed out and allow the
model to have about the same basic pitching moment at zero lift as the
airplane with the design airfoil.

The tip portions of the sweptback panels were provided with trimming
tips which were used in trimming out the pitching moments of the wing
and were held at a constant setting during flight. The aileron and
elevator control was provided by a set of controllers which extended
from approximately the midsection of the sweptback panels to the wing
tips. These surfaces were actuated in the same direction for elevator
control and differentially for aileron control. Approximately half
of the area of the controllers was attached to the trimming tips and
these portions of the controllers changed their position relative to
the wing in the same way as the trimming tips. Control was applied to

these outboard portions of the controllers by means of a direct linkage
from the inboard portion of the controllers. The wing was built
with $4.75^{\circ}$ washout at the wing tip as specified for the airplane.

The different tail configurations used on the model were as follows:
design tip tails, large tip tails, design tip tails plus large inboard
tails, and large tip tails plus large inboard tails. (See fig. 3.)

TESTS

Force Tests

Force tests were made with the flap up and flap down to determine
the static stability characteristics of the model in its design configu-
ration and with increased vertical-tail area. The configurations tested
in the Langley free-flight tunnel are listed in table II and are desig-
nated by the letters FFT. Also listed in table II are comparative con-
figurations tested at the National Research Council of Canada and are
designated by the letters NRCC. All the free-flight-tunnel tests were
made with trimming tips at $-20^{\circ}$, and the flap-down tests were made with
the canopies off. Results of tuft surveys indicated that considerable
turbulence occurred in the region of the canopies and directly behind
the canopies on the trailing edge of the wing. Since the maximum lift
coefficient was relatively low for the flap-down configuration and the
canopies showed a definite detrimental effect on the stall character-
istics, it was decided that all flap-down tests would be made with
canopies off to obtain as high a lift coefficient as possible. Aileron-
and rudder-effectiveness tests were made at angles of attack of $0^{\circ}$, $10^{\circ}$,
and $20^{\circ}$. All force tests were run at a dynamic pressure of 3.00 pounds
per square foot, which corresponds to an airspeed of about 34 miles per
hour at standard sea-level conditions and to a test Reynolds number
of 278,000 based on the mean aerodynamic chord of 0.87 foot.

Flight Tests

Flight tests were made to determine the general flying character-
istics of the model over a speed range corresponding to a lift-coefficient
range from 0.46 to 0.94 for center-of-gravity positions of 48- and
52-percent center-section chord for the flap-up configuration, and
from 0.63 to 1.43 for center-of-gravity positions of 47- and 52-percent
center-section chord for the flap-down configuration. Flights were made
with both the flap-up and flap-down conditions with the design tails,
large tip tails, and large tip tails plus large inboard tails. The flap-
up condition was also flown with the design tails and large inboard tails.
Table II shows the configurations tested with values of $C_{n_\beta}$ and $C_{l_\beta}$
corresponding to each configuration. Most of the flights were made with
trimming tips at $-20^{\circ}$ and elevators trimmed up $20^{\circ}$ with deflections of $\pm25^{\circ}$

and rudders trimmed at $0^\circ$ with deflection of $\pm 20^\circ$. The center trimmer
and outboard trimmers were changed to obtain trim of the model over the
lift-coefficient range. The flap-down flights were made with canopies
off and center trimmer at $0^\circ$. All flights were made with the aileron
and elevator control similar to that of the airplane where the wing
control surfaces act together for elevator control and differentially
for aileron control. The aileron and rudder control surfaces were
actuated simultaneously for flights where these controls were both used,
or ailerons-alone flights were made by switching out the rudder.

## Calculations

Calculations were made to determine the neutral-lateral-oscillatory-
stability boundary (R = 0) for the model in the flap-up and flap-down
configurations by the method described in reference 4. The roots of the
lateral-stability equations were used to determine the period and damping
data of the oscillatory mode and the damping data of the aperiodic modes
for the model in the flap-up and flap-down configurations with various
vertical-tail areas. Additional calculations were made to determine the
effect of reducing the yawing and rolling radii-of-gyration on the
period and damping of the lateral oscillation.

The aerodynamic and mass characteristics used in the calculations
are presented in table III. Values of $C_{n_\beta(\text{tail off})}$ and $C_{Y_\beta(\text{tail off})}$
were determined from force tests made in the Langley free-flight tunnel.
The tail-off values of $C_{n_r}$, $C_{l_r}$, $C_{l_p}$, $C_{n_p}$ were estimated from refer-
ence 5. The contributions of the tail to the stability derivatives were
estimated from the equations given in the footnote of table III and are
similar to those given in reference 6. The inclination of the principal
longitudinal axis above the flight path is expected to be lower for the
free-flight-tunnel model than for the airplane since the model has a
cambered airfoil section and would therefore attain a given lift coeffi-
cient at a lower angle of attack. The difference between the angle $\eta$
for the model and airplane, however, is not expected to be of great
importance since for this particular design the yawing and rolling radii-
of-gyration have about the same value, which results in the product-of-
inertia factor $K_{XZ}$ being small. When $K_{XZ}$ is small, the inclination
of the principal axis does not appreciably affect the R = 0 boundary.
The effect of this difference would be to make the airplane slightly
more stable than the model.

Calculations were made by the National Research Council of Canada
to determine the oscillatory stability and damping characteristics of
the airplane and the results were presented in reference 7. These
calculations indicated more stability than that obtained in the free-
flight-tunnel calculations. A comparison of the two sets of stability
derivatives showed considerable differences in some of the parameters.

For example, the NRCC calculations were made using a value of $C_{l_p}$ of the order of -0.60; whereas the free-flight-tunnel calculations were made using a value of $C_{l_p}$ of -0.30. This difference would account for some of the reasons why the NRCC boundary showed more stability than the free-flight-tunnel boundary.

## RESULTS AND DISCUSSION

### Force-Test Results

Longitudinal stability.- The results of the force tests made to determine the longitudinal stability characteristics of the free-flight-tunnel model are presented in figures 6 and 7. Also shown in these figures are data from the National Research Council of Canada for a $\frac{1}{8}$-scale model. The Canadian data were obtained at a dynamic pressure of 26.8 pounds per square foot which corresponds to an airspeed of about 102 miles per hour at standard sea-level conditions and to a test Reynolds number of 1,040,000 based on the mean aerodynamic chord of 1.09 feet.

The data of figure 6 show that the static longitudinal stability of the free-flight-tunnel model with flap up decreases with increasing lift coefficient so that there is a small amount of instability near the stall. The NRCC data, however, show an increase in stability with increasing lift coefficient with greater stability at the stall. The flap-down data of figure 7 show that the free-flight-tunnel model had an increase in stability with increasing lift coefficient; whereas the NRCC data show a decrease in stability at the high lift coefficients with instability occurring at the stall. The differences existing between the two sets of data are probably associated with the differences in the scale of tests, the different airfoil sections, and the different control settings on the models. An attempt was made to duplicate the results of the Canadian tests by using leading-edge slats and guide vanes on the free-flight-tunnel model. It was found, however, that these modifications had very little effect on the data and none of the modifications were incorporated in the model. The free-flight-tunnel model, therefore, does not represent the full-scale airplane with regard to static longitudinal stability if it is assumed that the higher-scale tests give a correct indication of the airplane characteristics.

Lateral stability.- The variations of the lateral-stability parameters $C_{Y_\beta}$, $C_{n_\beta}$, and $C_{l_\beta}$ with lift coefficient are presented in figures 8 and 9 for several free-flight-tunnel model configurations, together with data from the National Research Council of Canada for the design configuration. The NRCC lateral data were obtained at a dynamic pressure of 47.5 pounds per square foot which corresponds to an airspeed

of 136 miles per hour at standard sea-level conditions and to a test
Reynolds number of 1,390,000 based on the mean aerodynamic chord
of 1.09 feet.

The results of figure 8 show that the free-flight-tunnel model had
more directional stability and effective dihedral for the design con-
figuration with flap up than that obtained in the NRCC tests. The larger
value of $C_{n_\beta}$ for the free-flight-tunnel model was probably caused by
the cambered airfoil section and the different control settings.
Figure 8 also shows that as the vertical-tail area was increased, the
directional stability $C_{n_\beta}$ increased over the lift-coefficient range.
The positive effective dihedral $-C_{l_\beta}$ generally increased with increasing
tail area throughout the low and medium lift-coefficient range. For the
large tip tail configuration, however, a more rapid decrease in $-C_{l_\beta}$
was obtained at the higher lift coefficients.

The flap-down data of figure 9 show that the free-flight-tunnel
model had slightly higher $C_{n_\beta}$ over most of the lift-coefficient range
than was shown by the NRCC tests and that the variation of $C_{l_\beta}$ with
lift coefficient was much less for the free-flight model than for the
NRCC model over the lower lift-coefficient range. Increasing the vertical-
tail area increased both the positive effective dihedral $-C_{l_\beta}$ and the
directional-stability parameter $C_{n_\beta}$ as was the case for the flap-up
model.

Presented in figures 10 and 11 are the results of tests made to
determine the aileron and rudder effectiveness for the model in the
design configuration. These results show a decrease in control effective-
ness with increasing angle of attack. The aileron tests showed very
little adverse aileron yawing moments, but the rudder tests showed
relatively large adverse rolling moments.

### Flight-Test Results

Longitudinal stability.- The results of the flight tests showed
that the model in the flap-up configuration had satisfactory longitudinal
stability with the center-of-gravity position of 52-percent center-section
chord (12-percent static margin) over a speed range corresponding to a
range of lift coefficients from 0.46 to 0.94. At higher lift coeffi-
cients the model exhibited a nosing-up tendency as indicated by the
force-test results. Moving the center of gravity to 49-percent center-
section chord did not appreciably improve the stability at the stall.
In the flap-down configuration, the longitudinal stability of the model
was satisfactory over a range of lift coefficients from 0.63 to 1.43 for
center-of-gravity positions of 47-percent center-section chord (18-percent
static margin) and 52-percent center-section chord (12-percent static
margin).

Because, as previously mentioned, the Langley free-flight-tunnel force tests are not in agreement with the NRCC results with regard to static longitudinal stability near the stall, the dynamic behavior of the model near the stall is not expected to correspond to that of the full-scale airplane. In fact, on the basis of the force-test results the flap-up condition for the free-flight-tunnel model should represent the flap-down condition for the airplane and vice versa. It should therefore be expected that the longitudinal stability of the airplane will be satisfactory with flap up but unsatisfactory near the stall with flap down.

Lateral stability.- Flight tests to determine the lateral stability and control characteristics showed that in the design configuration the model had poor Dutch roll stability over the lift-coefficient range with the flap up or down. Flights with the design tail were generally fairly steady until the model was disturbed. Once an oscillation started, however, it was almost impossible to get the model settled down again and the flight usually ended with the model crashing into the wall. The lateral motions of the model in flight with the design tail arrangement are presented in figures 12(a) and 13(a) for flap up and flap down, respectively. The first flight record in figure 12(a) represents the flight characteristics of the model under more or less steady flight conditions and the second illustrates the type of motion resulting from a disturbance. The flap-down model showed about the same characteristics as the flap-up model. (See fig. 13(a).)

The results of calculations made to determine the dynamic lateral stability characteristics of the model (table IV and figs. 14 and 15) showed fairly good agreement with the flight-test results. These model results can be converted to full-scale results for this particular airplane by multiplying the model values by the factor $\sqrt{10}$. Plotted on figures 14 and 15 are the stability boundaries and the $C_{n_\beta}$ and $-C_{l_\beta}$ values of the model with the different tail configurations. It is seen that the point representing the flap-up model with the design tail is slightly on the unstable side of the $R = 0$ boundary and the point representing the flap-down model shows a very small amount of stability. The calculated damping results showed a period of 1.51 seconds and a time to double amplitude of 8.41 seconds (5.55 cycles) for the flap-up model at a lift coefficient of 0.60. With the flap down, the period of the oscillation was 2.09 seconds and the time to damp to one-half amplitude was 37.51 seconds (17.93 cycles) for a lift coefficient of 1.2.

Also plotted in figures 14 and 15 are the NRCC values of $C_{n_\beta}$ and $-C_{l_\beta}$ for purposes of comparison with the free-flight-tunnel data. From the results of these figures, it is seen that the NRCC points are in the unstable region of the $R = 0$ boundary. The oscillatory stability of the airplane is therefore expected to be somewhat worse than that of the model if it is assumed that the stability boundaries for the airplane are similar to those for the model and the NRCC static tests are representative of the airplane.

Flights made with increased tail size showed improved stability and control characteristics. As $C_{n_\beta}$ was increased, the oscillations generally became more heavily damped and flights became steadier. With the large tip tails, however, a moderate disturbance would still start an oscillation that was difficult to control. The flight records for the configuration with large tip tails (figs. 12(b) and 13(b)) show some improvement over the flight records of the design tail configuration. The flap-down data of figure 13(b) represent the type of motion resulting from a disturbance and show that this oscillation can be controlled. The results of figures 14 and 15 show this condition to be slightly unstable with flap up and slightly stable with flap down. The calculated damping results showed a period of 1.39 seconds and a time to double amplitude of 11.59 seconds (8.35 cycles) for the flap-up model at a lift coefficient of 0.60. With the flap down, the period of the oscillation was 1.74 seconds and the time to damp to one-half amplitude was 10.93 seconds (6.26 cycles) for a lift coefficient of 1.2.

The flap-up model was also tested with design tip tails and large inboard tails and showed about the same flight characteristics as with the large tip tails. Figure 14 shows that the point representing this configuration is slightly below the $R = 0$ boundary. The calculated damping showed a period of 1.31 seconds and a time to double amplitude of 21.60 seconds (16.50 cycles) for a lift coefficient of 0.60.

With the further increase in directional stability by the installation of the large tip tails plus the large inboard tails, the stability with flap up was improved but the model could still be disturbed so as to start an oscillation which was not very heavily damped. The flight record of figure 12(c) shows this condition to have about the same flight characteristics as figure 12(b) but the opinion of the pilot was that the configuration with large tip tails plus large inboard tails was the most stable for the flap-up conditions. The calculated stability for this condition showed a period of 1.16 seconds and a time to damp to one-half amplitude of 18.28 seconds (15.80 cycles) for a lift coefficient of 0.60.

With the large tip and inboard tails and flap down, the oscillation was difficult to start and once it was started it appeared to damp in two or three cycles. The flight record of figure 13(c) shows about the same results as the flap-up data of figure 12(c) but here again the flap-up flights were generally a little worse than the flap-down flights. The calculated stability for this condition showed a period of 1.58 seconds and a time to damp to one-half amplitude of 4.31 seconds (2.72 cycles) for a lift coefficient of 1.2.

It was found from the flight tests of all conditions that once an oscillation was started, the model was more difficult to control with coordinated ailerons and rudders than with ailerons alone. It has been found from previous experience in the free-flight tunnel that models with poor Dutch roll stability are more difficult to fly with combined

aileron and rudder control, probably because of too much favorable yaw
due to the rudder. The favorable yawing moment that occurs when the
rudders are deflected in the normal manner appears to help build up the
oscillation once the model is disturbed. Some flights were made with
rudders reversed and the results showed that flights were better than
those with rudder used in normal manner and were about as good as flights
with ailerons alone.

Presented in figure 16 are the calculated damping characteristics
of the airplane and the damping required by the U. S. Air Force (refer-
ence 8). It is seen that the flap-down configurations are slightly more
stable than the flap-up configurations but none of the configurations
meet the specified requirement.

From the results of the investigation it appears that fairly satis-
factory lateral flying characteristics could be obtained on this airplane
with a value of directional stability $C_{n_\beta}$ of at least 0.002. Good
flying characteristics could probably be obtained with a smaller value
of $C_{n_\beta}$ provided the positive effective dihedral $-C_{l_\beta}$ could be kept
small.


Comparison of Tailless Glider with Conventional-Type

Sweptback Airplane

A comparison of the calculated dynamic lateral stability character-
istics of the N.R.L. tailless glider with those of a conventional-type
sweptback fighter having a similar wing plan form and about the same
inclination of the longitudinal principal axis of inertia showed that
the tailless glider had poorer dynamic lateral stability. A comparison
of the mass and aerodynamic parameters showed a much larger value of
the damping-in-yaw parameter $C_{n_r}$ for the conventional type and a larger
value of the rolling radius-of-gyration factor $K_{X_0}$ for the all-wing
type. The smaller value of $C_{n_r}$ of the tailless glider is due partly
to the shorter tail length which is inherent in this type of design,
and the larger value of $K_{X_0}$ of the tailless glider is caused by the
load distribution along the wing typical of all-wing airplanes. An all-
wing airplane usually has a mass distribution similar to that of a
conventional-type airplane with wing-tip tanks. The results of refer-
ences 9 to 11 show that such a mass distribution can be detrimental to
dynamic lateral stability. In order to illustrate the importance of $K_{X_0}$
on the lateral stability characteristics in this particular case,
calculations were made to determine the period and damping of the lateral
oscillation for the model with the value of the rolling radius-of-
gyration factor $K_{X_0}$ reduced 25 and 50 percent. The yawing radius-of-
gyration factor $K_{Z_0}$ was reduced simultaneously with $K_{X_0}$ because in
a practical case reducing $K_{X_0}$ cannot be accomplished without also

reducing $K_{Z_O}$. Results of these calculations (presented in table IV)
showed large improvements in the damping characteristics. The calcula-
tions show that the lateral oscillation was made stable for the
N.R.L. tailless glider in the design condition with flap up by reducing
the yawing and rolling radii of gyration. The value of these parameters
required for enough stability to meet the Air Force specification, how-
ever, would be impractical to attain for this type of design. This
effect of mass distribution on lateral stability characteristics is
covered more fully in references 9 to 11.

Additional calculations were also made to determine the effect on
lateral stability of increasing $C_{n_r}$ to a value corresponding to that
of a conventional airplane. It was found that this increase in $C_{n_r}$
had a stabilizing effect on the lateral stability characteristics but
was not as great as the stabilizing effect caused by reducing the value
of $K_{X_O}$ to that of a conventional airplane, previously discussed in the
preceding paragraph. Increasing $C_{n_r}$ to a value corresponding to that
of a conventional airplane corresponded to about a 20-percent decrease
in the value of $K_{X_O}$.

CONCLUDING REMARKS

The following conclusions were drawn from the results of the free-
flight-tunnel stability and control investigation on a $\frac{1}{10}$-scale model
of a Canadian tailless glider:

1. On the basis of comparison of the free-flight-tunnel tests and
higher-scale NRCC static tests it is expected that the longitudinal
stability of the airplane will be satisfactory with flap up but unsatis-
factory near the stall with flap down.

2. The airplane is expected to have unsatisfactory lateral stability
and control characteristics in the design configuration with the flap
up and flap down. The model flights showed very low damping of the
lateral oscillations.

3. Increasing the vertical-tail area improved the lateral stability
of the model and it appeared that a value of $C_{n_\beta}$ of at least 0.002 per
degree would probably be necessary for satisfactory lateral flying
characteristics.

4. A comparison of the calculated dynamic lateral stability charac-
teristics of the N.R.L. tailless glider with those of a conventional-
type sweptback airplane having a similar wing plan form and about the

same inclination of the principal longitudinal axis of inertia showed
that the tailless glider had poorer lateral stability because of the
relatively larger radius of gyration in roll and the smaller damping-
in-yaw factor $C_{n_r}$.

Langley Aeronautical Laboratory
    National Advisory Committee for Aeronautics
        Langley Air Force Base, Va.

Joseph L. Johnson
Aeronautical Research Scientist

Approved:

Thomas A. Harris
Chief of Stability Research Division

jjm

## REFERENCES

1. Shortal, Joseph A., and Osterhout, Clayton J.:  Preliminary Stability and Control Tests in the NACA Free-Flight Wind Tunnel and Correlation with Full-Scale Flight Tests.  NACA TN No. 810, 1941.

2. Shortal, Joseph A., and Draper, John W.:  Free-Flight-Tunnel Investigation of the Effect of the Fuselage Length and the Aspect Ratio and Size of the Vertical Tail on Lateral Stability and Control.  NACA ARR No. 3D17, 1943.

3. National Advisory Committee for Aeronautics:  Aerodynamic Characteristics of Airfoils.  NACA Rep. No. 315, 1929.

4. Zimmerman, Charles H.:  An Analysis of Lateral Stability in Power-Off Flight with Charts for Use in Design.  NACA Rep. No. 589, 1937.

5. Toll, Thomas A., and Queijo, M. J.:  Approximate Relations and Charts for Low-Speed Stability Derivatives of Swept Wings.  NACA TN No. 1581, 1948.

6. Bamber, Millard J.:  Effect of Some Present-Day Airplane Design Trends on Requirements for Lateral Stability.  NACA TN No. 814, 1941.

7. Rosenthal, G., and Callan, M. M.:  Model Tests on the Static Lateral Stability of the N.R.L. Tailless Glider and Calculated Lateral Characteristics.  NRCC (Ottawa) Lab. Note AE-5-47, Sept. 17, 1947.

8. Anon.:  U. S. Air Force Specification for Flying Qualities of Piloted Airplanes.  No. 1815-B, June 1948.

9. Campbell, John P., and Seacord, Charles L., Jr.:  The Effect of Mass Distribution on the Lateral Stability and Control Characteristics of an Airplane as Determined by Tests of a Model in the Free-Flight Tunnel.  NACA Rep. No. 769, 1943.

10. Sternfield, Leonard:  Some Considerations of the Lateral Stability of High-Speed Aircraft.  NACA TN No. 1282, 1947.

11. Campbell, John P., and Toll, Thomas A.:  Factors Affecting Lateral Stability and Controllability.  NACA RM No. L8A28a, 1948.

TABLE I

DIMENSIONAL AND MASS CHARACTERISTICS OF N.R.L. TAILLESS GLIDER

AND SCALED-UP CHARACTERISTICS OF $\frac{1}{10}$-SCALE MODEL TESTED

IN LANGLEY FREE-FLIGHT TUNNEL

| | Scaled-up | Full-scale |
|---|---|---|
| Weight, lb . . . . . . . . . . . . . . . . . . . . . . . | 5060 | 3850 |
| Relative density factor, $\mu$, $m/\rho Sb$ . . . . . . . . . | 3.786 | 2.88 |
| **Wing:** | | |
| Area, sq ft . . . . . . . . . . . . . . . . . . . . | 373.5 | 373.5 |
| Span, ft . . . . . . . . . . . . . . . . . . . . . | 46.67 | 46.67 |
| Aspect ratio . . . . . . . . . . . . . . . . . . . . | 5.84 | 5.84 |
| Sweepback, c/4, deg . . . . . . . . . . . . . . . . | 39.4 | 39.4 |
| Dihedral, deg (outer panels) . . . . . . . . . . | -2.8 | -2.0 |
| Taper ratio, Tip chord/Center-section chord . . . | 0.323 | 0.323 |
| Washout, deg . . . . . . . . . . . . . . . . . . . | 4.75 | 4.75 |
| M.A.C., ft . . . . . . . . . . . . . . . . . . . . | 8.70 | 8.70 |
| Location behind L.E. center-section chord . . . | 3.40 | 3.40 |
| Root chord, ft . . . . . . . . . . . . . . . . . . | 10.32 | 10.32 |
| Tip chord, ft . . . . . . . . . . . . . . . . . . | 3.33 | 3.33 |
| Wing loading, W/S, lb/sq ft . . . . . . . . . . . | 13.55 | 10.30 |
| **Flap:** | | |
| Span, ft . . . . . . . . . . . . . . . . . . . . . | 19.03 | 19.03 |
| Chord, ft . . . . . . . . . . . . . . . . . . . . . | 2.580 | 2.580 |
| Hinge line, percent center-section chord . . . . | 70.00 | 70.00 |
| Deflection, deg . . . . . . . . . . . . . . . . . | 60.00 | 60.0 longitudinal 45.0 lateral |
| **Vertical-tail surfaces:** | | |
| **Design tail:** | | |
| Total area (2 tails), sq ft . . . . . . . . . . . | 12.00 | 12.00 |
| Rudder area (2 tails), sq ft . . . . . . . . . . | 4.21 | 4.21 |
| Section . . . . . . . . . . . . . . . . . . . . . | NACA 0012 | NACA 0012 |
| Aspect ratio . . . . . . . . . . . . . . . . . . . | 3.5 | 3.5 |
| Maximum deflection . . . . . . . . . . . . . . . | 20° in, 20° out | 22° in, 38° out |
| **FFT large tail (tip or inboard):** | | |
| Total area (2 tails), sq ft . . . . . . . . . . | 30.00 | ------------------- |
| Rudder area (2 tails), sq ft . . . . . . . . . | 15.00 | ------------------- |
| Section . . . . . . . . . . . . . . . . . . . . . | NACA 4306 | ------------------- |
| Aspect ratio . . . . . . . . . . . . . . . . . . . | 2.0 | ------------------- |
| Maximum deflection . . . . . . . . . . . . . . . | 20° in, 20° out | ------------------- |
| **Controllers:** | | |
| Total area, sq ft . . . . . . . . . . . . . . . . | 10.45 | 10.45 |
| Span, ft (1) . . . . . . . . . . . . . . . . . . . | 8.17 | 8.17 |
| Chord, ft (constant) . . . . . . . . . . . . . . | 1.28 | 1.28 |
| **Trimming tips:** | | |
| Total area, sq ft . . . . . . . . . . . . . . . | 18.68 | 18.68 |
| Span, ft (1) . . . . . . . . . . . . . . . . . . . | 4.08 | 4.08 |
| **Center-of-gravity location:** | | |
| Percent center-section chord . . . . . . . . . . | 52.00 (force test) 47.0 to 52.0 (flight test) | 52.00 |
| **Moments of inertia:** | | |
| $I_X$, slug-ft$^2$ . . . . . . . . . . . . . . . . . | 14,700 | 9,500 |
| $I_Z$, slug-ft$^2$ . . . . . . . . . . . . . . . . . | 16,600 | 11,500 |
| $I_Y$, slug-ft$^2$ . . . . . . . . . . . . . . . . . | 3,150 | 2,500 |
| **Radius of gyration to wing span:** | | |
| $k_{X_0}/b$ . . . . . . . . . . . . . . . . . . . . | 0.207 | 0.191 |
| $k_{Z_0}/b$ . . . . . . . . . . . . . . . . . . . . | .220 | .210 |
| $k_{Y_0}/b$ . . . . . . . . . . . . . . . . . . . . | .096 | .088 |

TABLE II

VERTICAL-TAIL CONFIGURATIONS USED ON $\frac{1}{10}$-SCALE MODEL

OF N.R.L. TAILLESS GLIDER TESTED IN

LANGLEY FREE-FLIGHT TUNNEL

CONFIDENTIAL

| Configuration | Tail area, $S_t/S_w$ total | $C_{n_\beta}$ (per deg) | $-C_{l_\beta}$ (per deg) |
|---|---|---|---|
| Flap-up configuration, $C_L = 0.6$: | | | |
| Tail off, FFT | 0 | 0.0006 | 0.00075 |
| Tail off, NRCC | 0 | .00033 | .00117 |
| Design tip tail, FFT | 0.032 (2 tails) | .00095 | .00125 |
| Design tip tail, NRCC | .032 (2 tails) | .00050 | .00125 |
| Large tip tail, FFT | .08 (2 tails) | .00115 | .00145 |
| Design tip tail plus large inboard tail, FFT | .112 (4 tails) | .00132 | .0016 |
| Large tip tail plus large inboard tail, FFT | .16 (4 tails) | .00175 | .0020 |
| | | | |
| Flap-down configuration, $C_L = 1.2$: | | | |
| Design tip tail, FFT | .032 (2 tails) | .00090 | .00095 |
| Design tip tail, NRCC | .032 (2 tails) | .00090 | .00175 |
| Large tip tail, FFT | .08 (2 tails) | .00140 | .00130 |
| Large tip tail plus large inboard tail, FFT | .16 (4 tails) | .0018 | .00135 |

CONFIDENTIAL

NACA

TABLE III

STABILITY DERIVATIVES AND MASS CHARACTERISTICS USED

IN STABILITY CALCULATIONS

| Items | Flap-up condition | Flap-down condition |
|---|---|---|
| $W$, lb | 5.06 | 5.06 |
| $S$, ft$^2$ | 3.735 | 3.735 |
| $b$, ft | 4.667 | 4.667 |
| $\rho$ | 0.00238 | 0.00238 |
| $\mu_b$ | 3.786 | 3.786 |
| $K_X$ | 0.207 | 0.207 |
| $K_Z$ | 0.220 | 0.220 |
| $K_{XZ}$ | 0.00107 | 0.000695 |
| $l/b$ | 0.130 | 0.130 |
| $\bar{z}/b$ | 0 | 0 |
| $C_L$ | 0.60 | 1.20 |
| $\alpha$, deg | 8.0 | 4.0 |
| $\epsilon$, deg | -3.2 | -3.2 |
| $\eta$, deg | 11.2 | 7.2 |
| $\gamma$, deg | -11.2 | -10.4 |
| $C_{Y_p}$, per radian | 0 | 0 |
| $C_{Y_r}$, per radian | 0 | 0 |
| $C_{Y_\beta}$, per radian | $-0.0458 + C_{Y_{\beta(tail)}}$ | $-0.0458 + C_{Y_{\beta(tail)}}$ |
| [a]$C_{n_\beta}$, per radian | $0.0344 + C_{n_{\beta(tail)}}$ | $0.0344 + C_{n_{\beta(tail)}}$ |
| [a]$C_{l_p}$, per radian | $-0.30 + C_{l_{p(tail)}}$ | $-0.30 + C_{l_{p(tail)}}$ |
| [a]$C_{n_p}$, per radian | $-0.055 + C_{n_{p(tail)}}$ | $-0.055 + C_{n_{p(tail)}}$ |
| [a]$C_{l_r}$, per radian | $0.10 + C_{l_{r(tail)}}$ | $0.20 + C_{l_{r(tail)}}$ |
| [a]$C_{n_r}$, per radian | $-0.016 + C_{n_{r(tail)}}$ | $-0.025 + C_{n_{r(tail)}}$ |
| $C_{Y_{\beta(tail)}}$, per radian | [b]Variable | [b]Variable |

[a]Tail contributions are determined from the following equations:

$$C_{n_{\beta(tail)}} = -\frac{l}{b} C_{Y_{\beta(tail)}}$$

$$C_{l_{p(tail)}} = 2\left(\frac{\bar{z}}{b} - \frac{l}{b}\sin\alpha\right)^2 C_{Y_{\beta(tail)}}$$

$$C_{n_{p(tail)}} = C_{l_{r(tail)}} = -2\frac{l}{b}\left(\frac{\bar{z}}{b} - \frac{l}{b}\sin\alpha\right) C_{Y_{\beta(tail)}}$$

$$C_{n_{r(tail)}} = 2\left(\frac{l}{b}\right)^2 C_{Y_{\beta(tail)}}$$

CONFIDENTIAL

[b]Varied systematically as independent variable.

CONFIDENTIAL

TABLE IV

CALCULATED PERIOD AND DAMPING DATA FOR $\frac{1}{10}$-SCALE MODEL

OF N.R.L. TAILLESS GLIDER

| Configuration | $C_L$ | $C_{n_\beta}$ (per deg) | $-C_{l_\beta}$ (per deg) | Tail | Oscillatory mode | | | | | Aperiodic modes | | | |
|---|---|---|---|---|---|---|---|---|---|---|---|---|---|
| | | | | | | | | | | Rolling | | Spiral | |
| | | | | | Period | $T_{1/2}$ (sec) | $T_2$ (sec) | $C_{1/2}$ (cycles) | $C_2$ (cycles) | $T_{1/2}$ (sec) | $T_2$ (sec) | $T_{1/2}$ (sec) | $T_2$ (sec) |
| Flap up | 0.60 | 0.00095 | 0.00125 | Design tip | 1.514 | ------ | 8.41 | ----- | 5.55 | 0.1410 | -- | 51.75 | ---- |
| Do--------- | -do- | .00115 | .00145 | Large tip | 1.39 | ------ | 11.59 | ----- | 8.35 | .1380 | -- | 30.10 | ---- |
| Do--------- | -do- | .00132 | .0016 | Design tip plus large inboard | 1.312 | ------ | 21.60 | ----- | 16.50 | .1365 | -- | 22.90 | ---- |
| Do--------- | -do- | .00175 | .0020 | Large tip plus large inboard | 1.157 | 18.28 | ----- | 15.80 | ----- | .1328 | -- | 13.60 | ---- |
| Flap down | 1.2 | .00090 | .00095 | Design tip | 2.09 | 37.51 | ----- | 17.93 | ----- | .1921 | -- | ----- | 3.59 |
| Do--------- | -do- | .00140 | .00130 | Large tip | 1.744 | 10.93 | ----- | 6.26 | ----- | .1840 | -- | ----- | 3.70 |
| Do--------- | -do- | .0018 | .00135 | Large tip plus large inboard | 1.58 | 4.31 | ----- | 2.72 | ----- | .1829 | -- | ----- | 3.50 |
| Flap up $k_{X_o}/b$, $k_{Z_o}/b$ reduced 25 percent | .60 | .00095 | .00125 | Design tip | 1.136 | 6.61 | ----- | 5.82 | ----- | .0857 | -- | 47.60 | ----- |
| $k_{X_o}/b$, $k_{Z_o}/b$ reduced 50 percent | .60 | .00095 | .00125 | Design tip | .759 | 1.024 | ----- | 1.35 | ----- | .0408 | -- | 44.60 | ----- |

CONFIDENTIAL

NACA

CONFIDENTIAL

Reference axis

Principal axis

$\chi$

Flight path

$\theta$  $\propto$

$\eta$

$\epsilon$

$\gamma$

Horizontal axis

$Z$

NACA
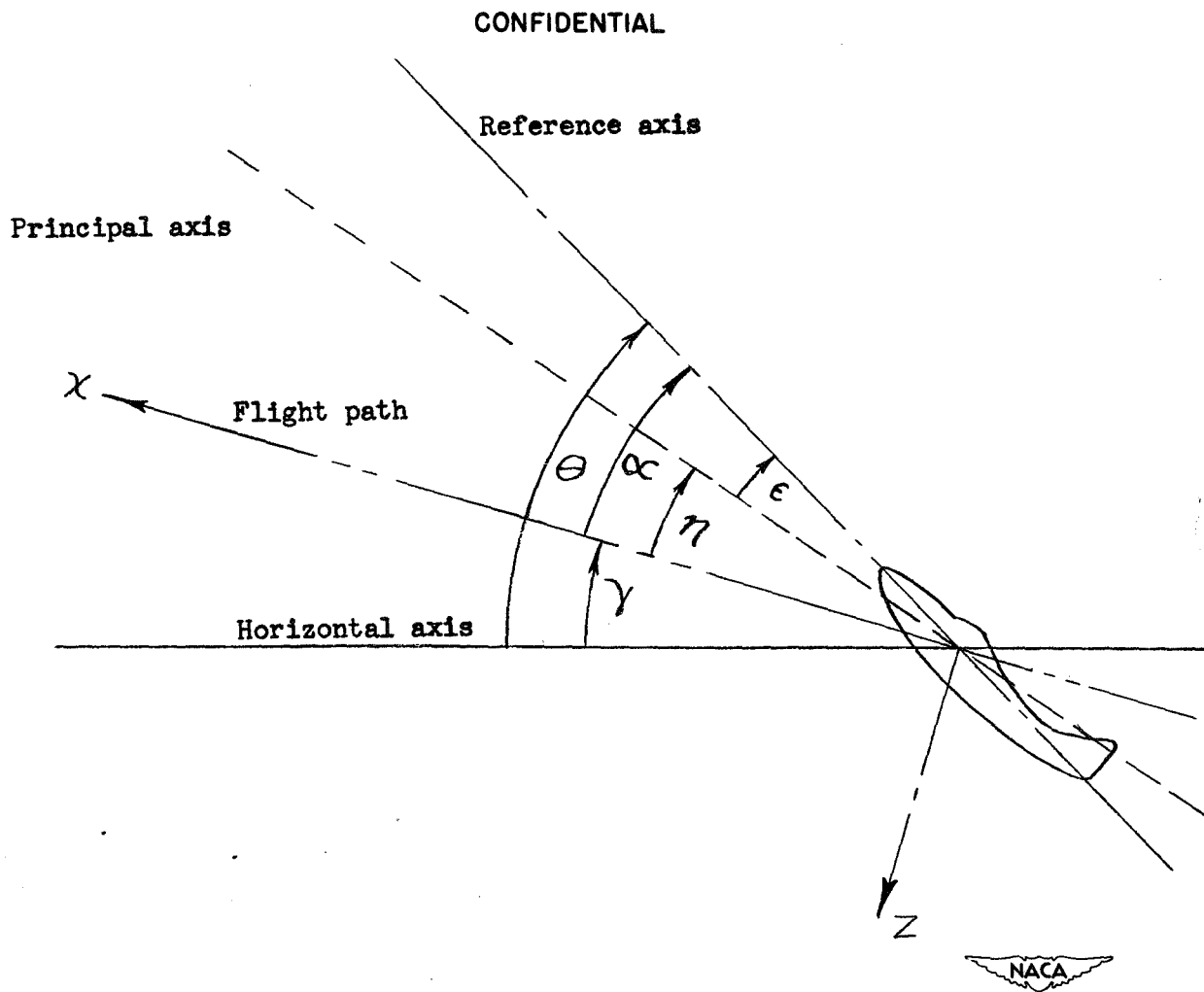
Figure 1.— System of axes and angular relationship in flight.  Arrows
indicate positive direction of angles.  $\eta = \theta - \gamma - \epsilon$.

CONFIDENTIAL

**CONFIDENTIAL**
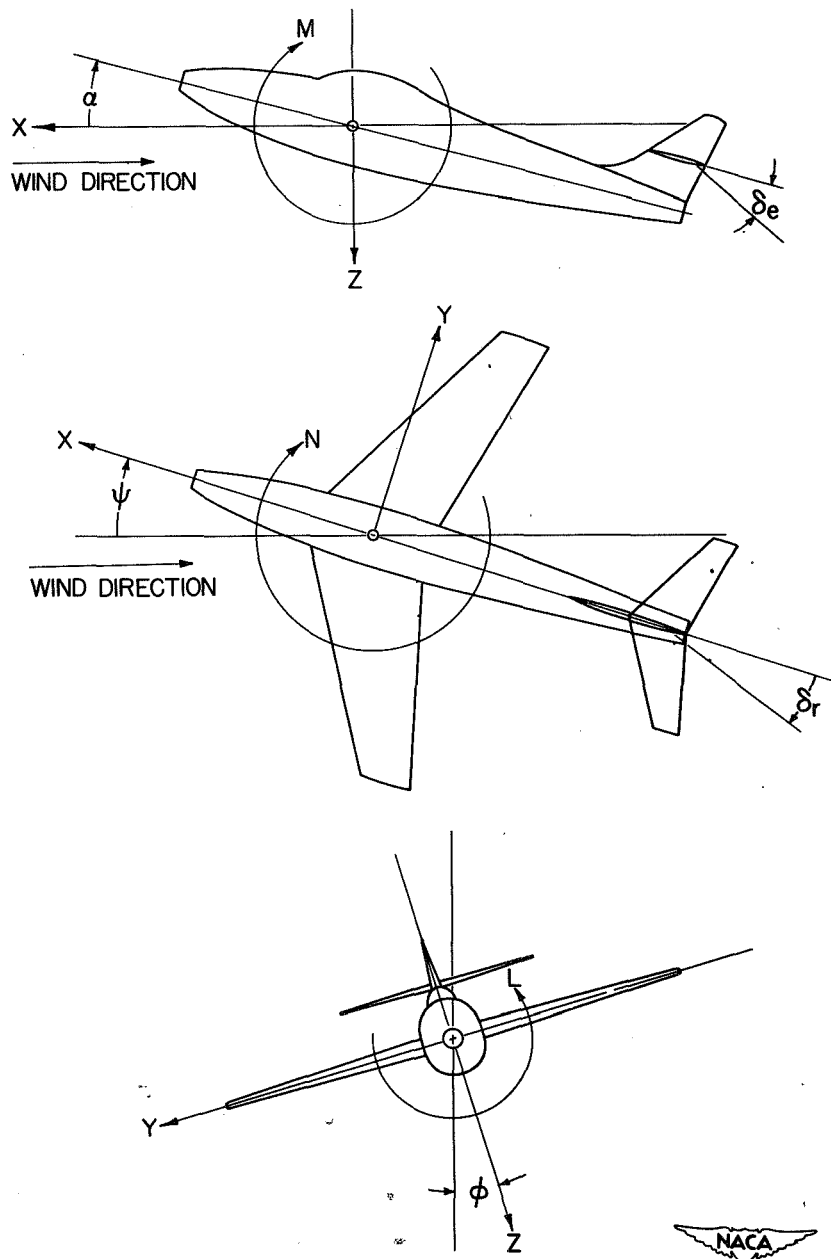
Figure 2.— The stability system of axes. Arrows indicate positive
directions of moments, forces, and control—surface deflections.
This system of axes is defined as an orthogonal system having
their origin at the center of gravity and in which the Z—axis
is in the plane of symmetry and perpendicular to the relative
wind, the X—axis is in the plane of symmetry and perpendicular
to the Z—axis, and the Y—axis is perpendicular to the plane of
symmetry.                           **CONFIDENTIAL**

CONFIDENTIAL
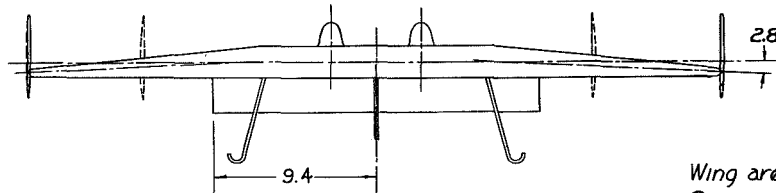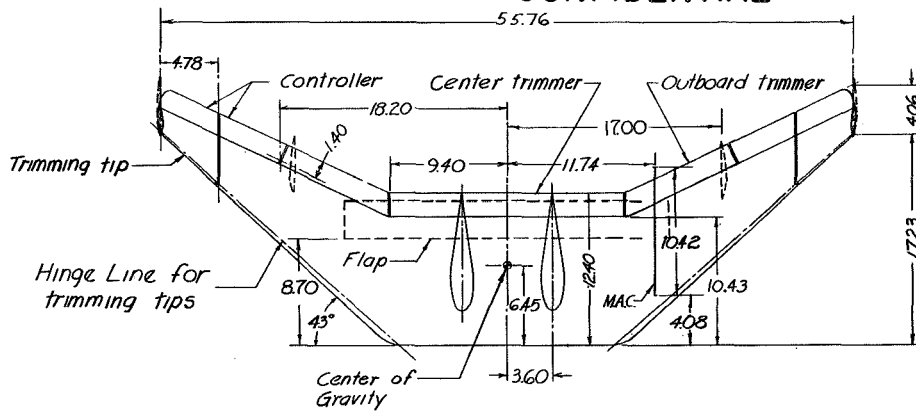


Wing area 3.73 ft²
Span 4.64 ft
Aspect ratio 5.83 ft
Taper ratio 0.323
C.G. Location 52%
center section chord

Design tail area .032 $S_w$ (2 tails)
aspect ratio 3.5
FFT large tail area .080 $S_w$ (2 tails
aspect ratio 2.0
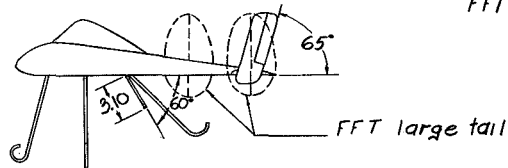
Figure 3.— Three—view drawing of a $\frac{1}{10}$—scale model of N.R.L. tailless glider used in the Langley free—flight—tunnel investigation. All dimensions in inches. CONFIDENTIAL
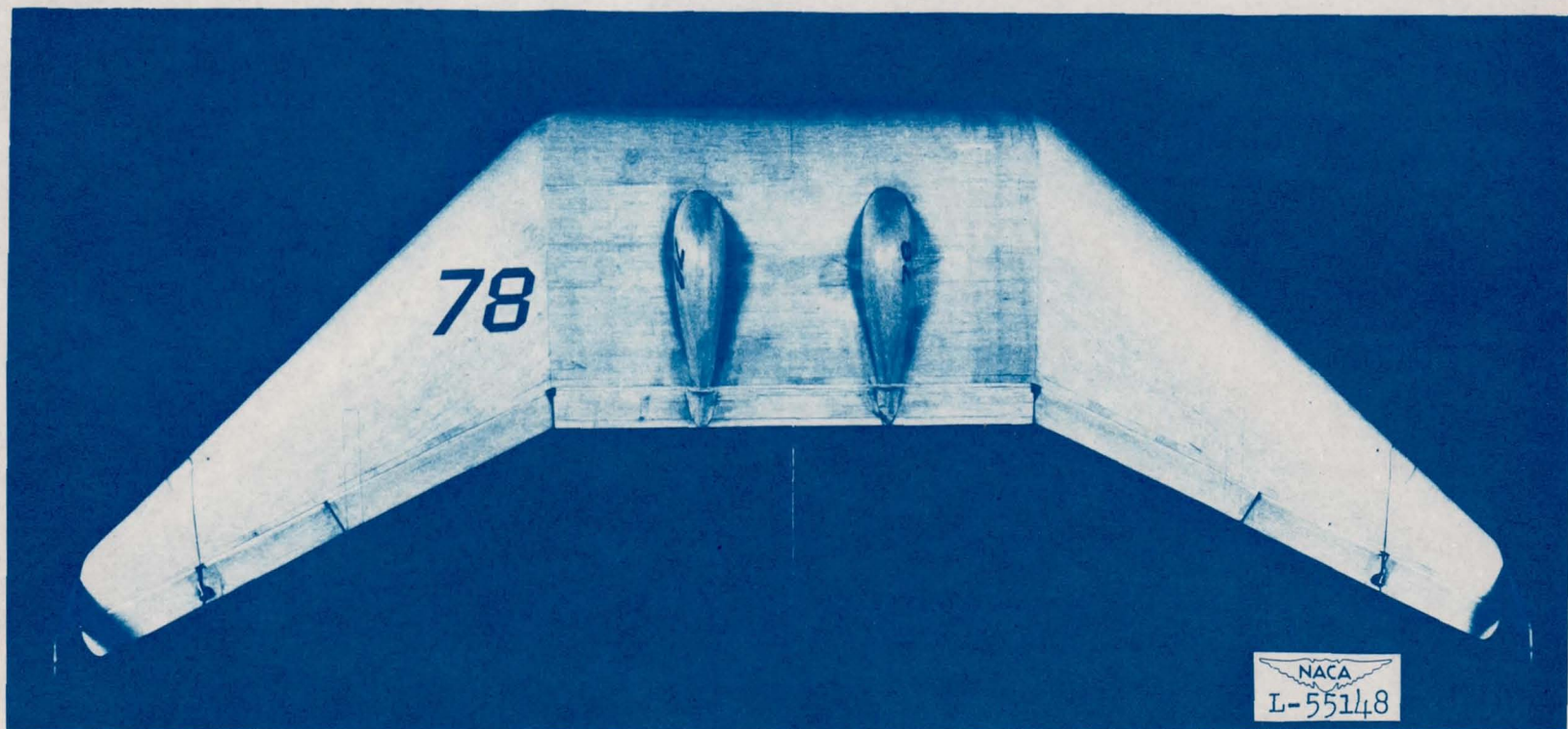
Figure 4.— Top view of a $\frac{1}{10}$-scale model of N.R.L. tailless glider tested in Langley free-flight tunnel.
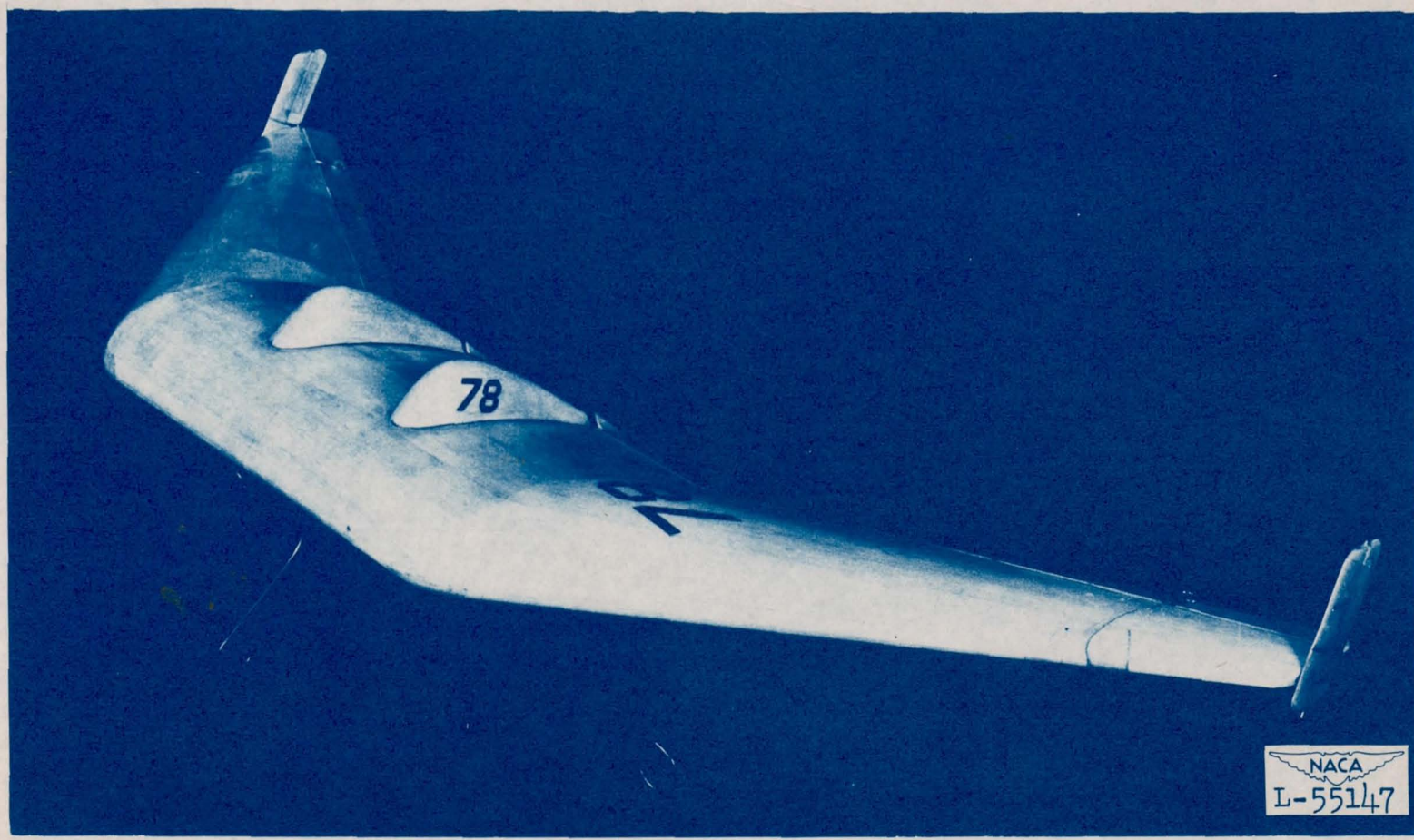
Figure 5.— Three—quarter front view of $\frac{1}{10}$—scale model of N.R.L. tailless glider tested in Langley free—flight tunnel.

CONFIDENTIAL

| | Source | $\delta_c$ | Trimmers Center | Outboard | Trimming Tips |
|---|---|---|---|---|---|
| ◯——— | FFT | 0 | 0 | 0 | 0 |
| ☐——— | FFT | -20 | -20 | -20 | -20 |
| △—·—· | NRCC | 0 | --- | --- | 0 |
| ◁—··— | NRCC | -15 | --- | --- | -15 |

Pitching · moment coefficient, $C_m$

.10

0

-.10

Drag coefficient, $C_D$

Lift coefficient, $C_L$

.4

.3

.2

.1

0

1.4

1.2

1.0

.8

.6

.4

.2

0

0    4    8    12    16    20    24

Angle of attack, $\alpha$, deg

.10    0    -.10

Pitching · moment coefficient, $C_m$

NACA
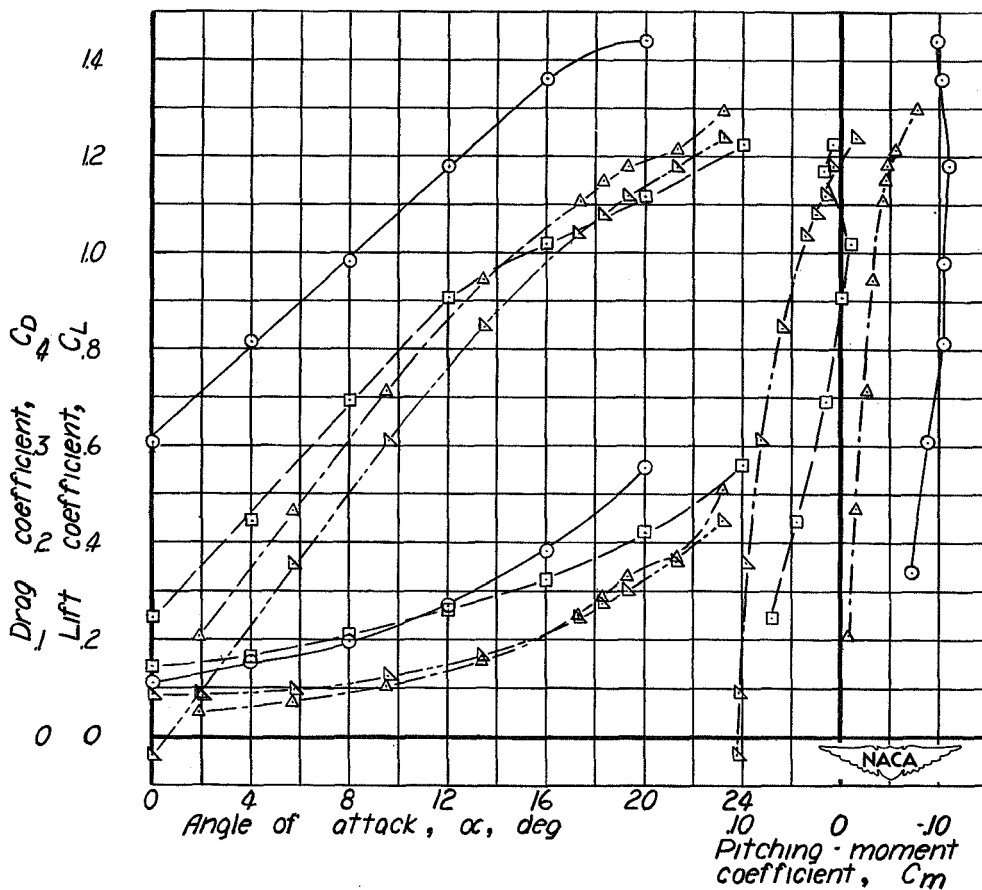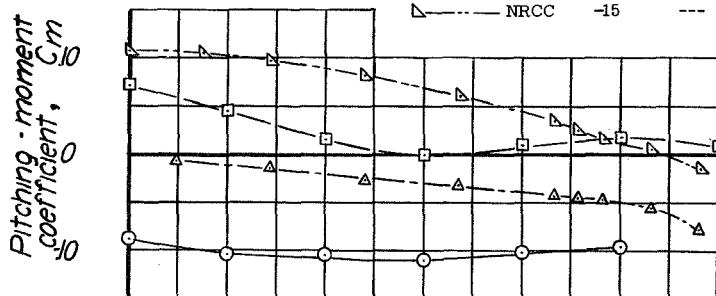
Figure 6.— Lift, drag, and pitching—moment characteristics of $\frac{1}{10}$—scale model of N.R.L. tailless glider tested in Langley free—flight tunnel compared with similar data from NRCC. Center of gravity = 52.0—percent center—section chord; $\psi$ = 0; $\delta_r$ = 0; $\delta_f$ = 0; q = 3.00 pounds/square foot for free—flight—tunnel data and 26.8 pounds/square foot for NRCC data.

CONFIDENTIAL

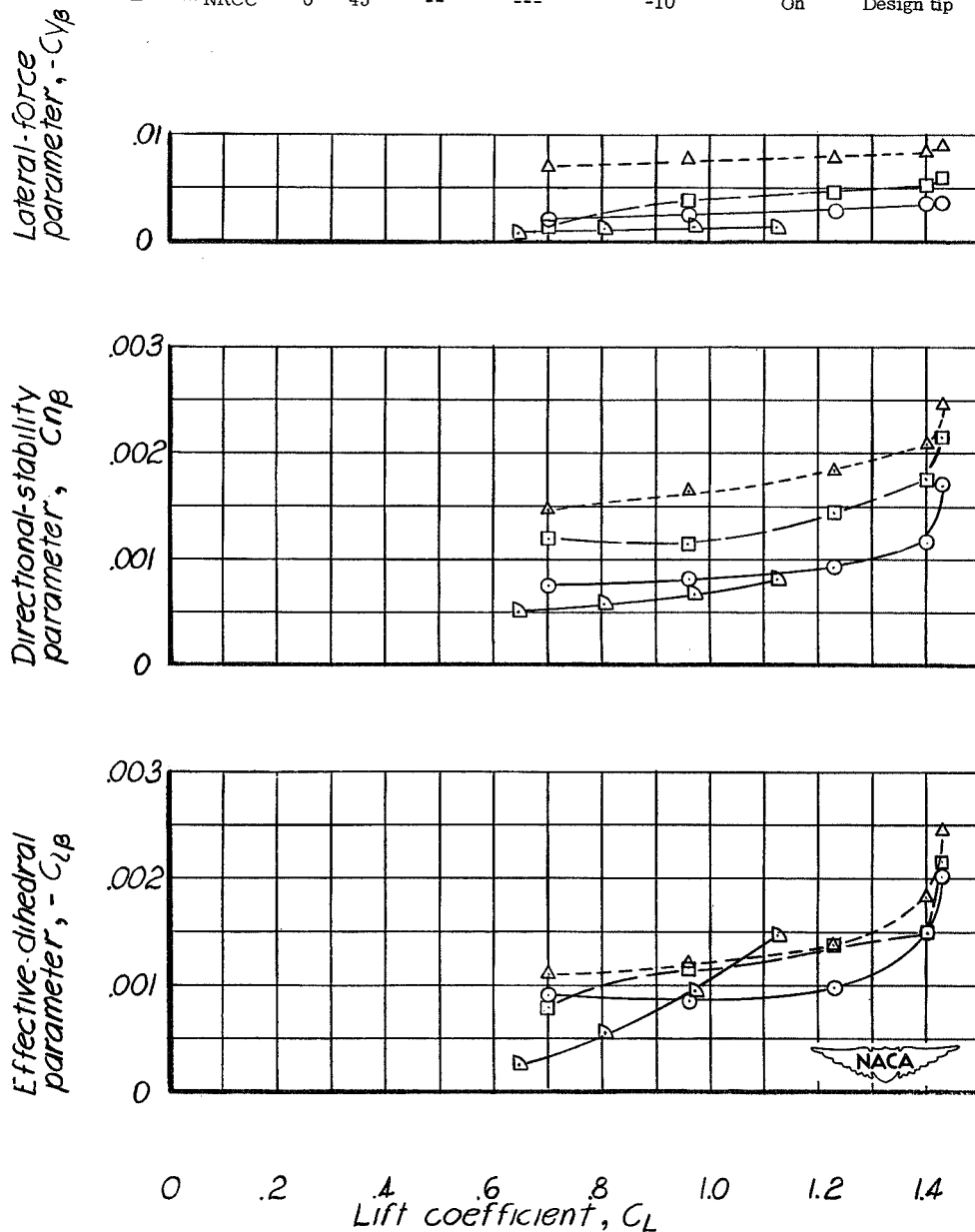Figure 7.— Lift, drag, and pitching—moment characteristics of $\frac{1}{10}$—scale model of N.R.L. tailless glider with flap deflected tested in the Langley free—flight tunnel compared with similar data from NRCC. Center of gravity = 52.0—percent center—section chord; $\psi$ = 0; $\delta_r$ = 0; q = 3.00 pounds/square foot for free—flight—tunnel data and 26.8 pounds/square foot for NRCC data.

CONFIDENTIAL

| Source | $\delta_c$ | Center | Outboard | Trimming tip | Tail |
|---|---|---|---|---|---|
| O———FFT | -20 | -20 | -20 | -20 | Design tip |
| □— —FFT | -20 | -20 | -20 | -20 | Large tip |
| ◇-----FFT | -20 | -20 | -20 | -20 | Design tail + large inboard |
| △-------FFT | -20 | -20 | -20 | -20 | Large tip + large inboard |
| ▷—··—FFT | -20 | -20 | -20 | -20 | Off |
| ▷———NRCC | 0 | --- | --- | --- | Design tip |
| △—··—NRCC | 0 | --- | --- | --- | Off |
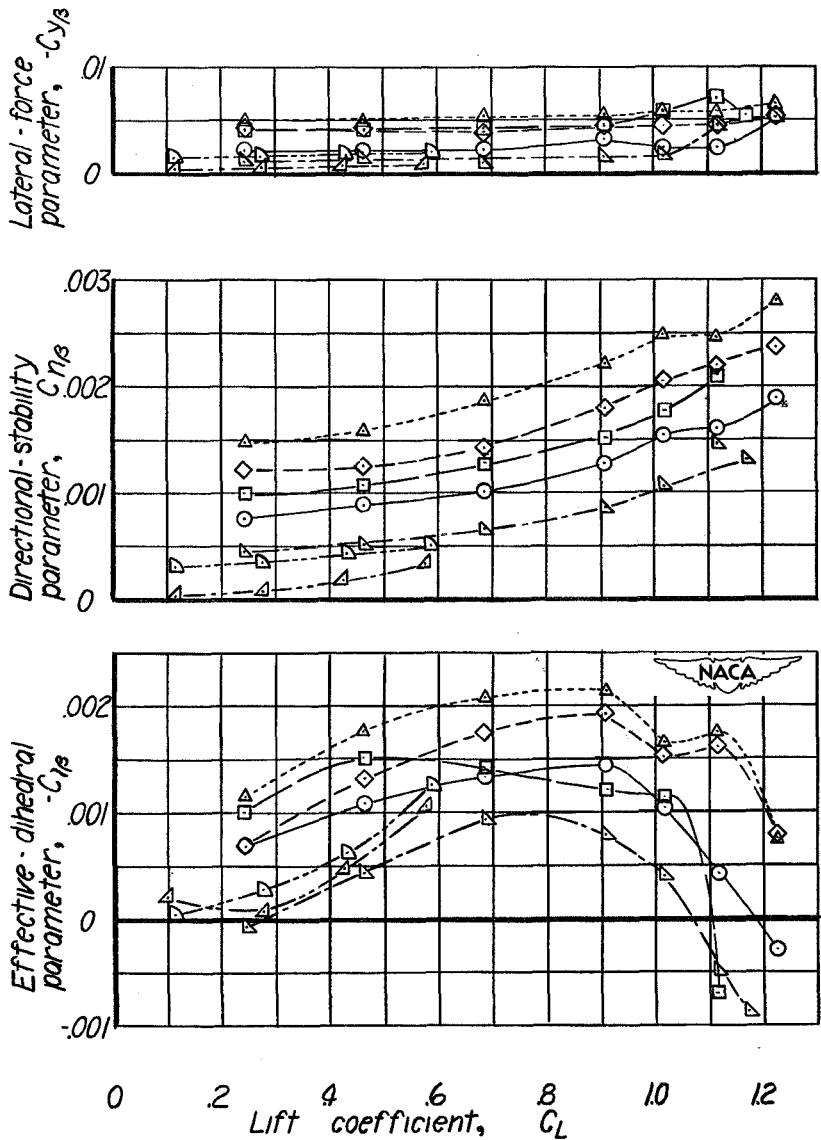


Figure 8.— Lateral stability characteristics of $\frac{1}{10}$— scale model of N.R.L. tailless glider tested in Langley free—flight tunnel compared with the data of the NRCC. Center of gravity = 52—percent center—section chord for free—flight—tunnel data and 51.0—percent center—section chord for NRCC data. $\delta_r = 0$; $\delta_f = 0$; q = 3.00 pounds/square foot for free—flight—tunnel data and 47.5 pounds/square foot for NRCC data.

CONFIDENTIAL

**CONFIDENTIAL**

| | Source | $\delta_c$ | $\delta_f$ | Trimmers Center | Outboard | Trimming Tip | Canopies | Tail |
|---|---|---|---|---|---|---|---|---|
| ○—— | FFT | -20 | 60 | 0 | -20 | -20 | Off | Design tip |
| □— — — | FFT | -20 | 60 | 0 | -20 | -20 | Off | Large tip |
| △- - - - | FFT | -20 | 60 | 0 | -20 | -20 | Off | Large tip + large inboard |
| ◁—— | NRCC | 0 | 45 | -- | --- | -10 | On | Design tip |



Figure 9.— Lateral stability characteristics of $\frac{1}{10}$—scale model of N.R.L. tailless glider with flap deflected tested in Langley free-flight tunnel and compared with data of NRCC. Center of gravity = 52.0—percent center—section chord for free—flight—tunnel data and 51.0—percent center—section chord for NRCC data. $\delta_r$ = 0; q = 3.00 pounds/square foot for free—flight—tunnel data and 47.5 pounds/square foot for NRCC data.
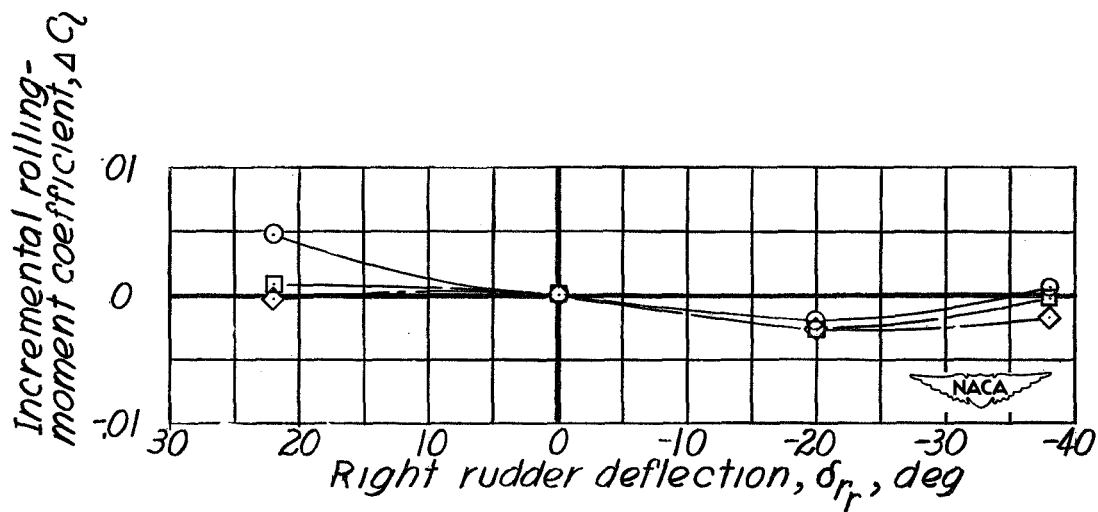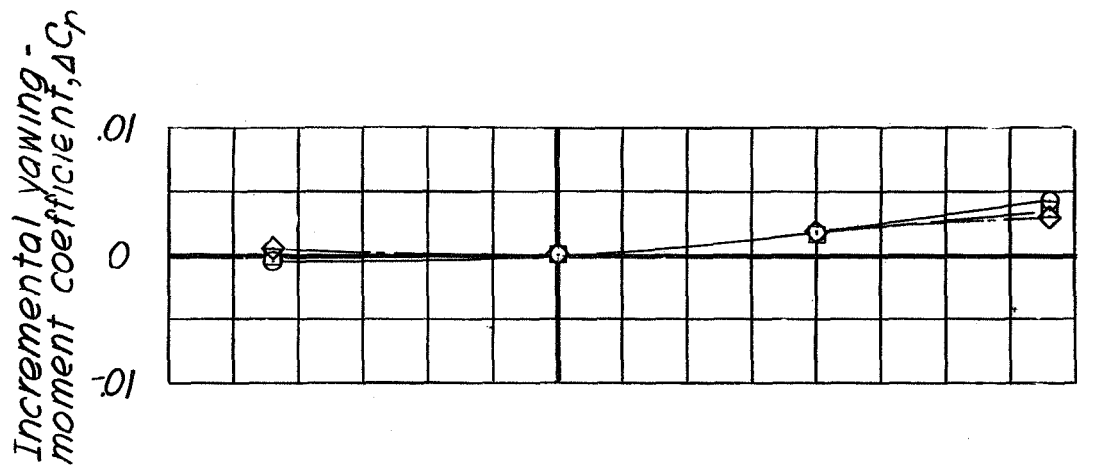
**CONFIDENTIAL**
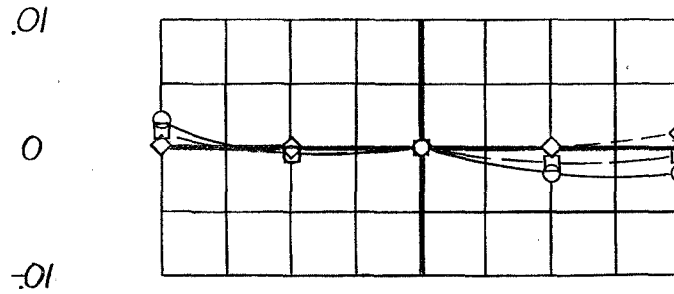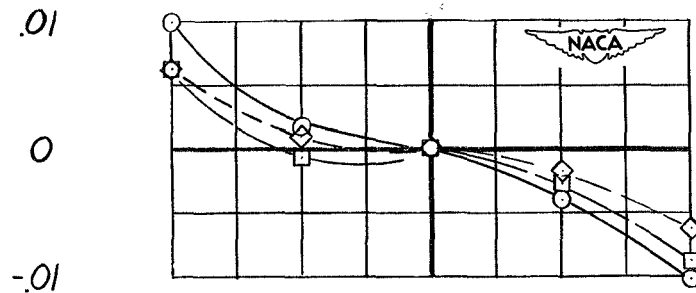
Figure 10.— Variation of aileron effectiveness with angle of attack for $\frac{1}{10}$— scale model of N.R.L. tailless glider tested in Langley free-flight tunnel. Center of gravity = 52.0—percent center-section chord; q = 3.00 pounds/square foot; $\delta_{a_L}$ = —20°; design vertical tail; Trimmers = —20°; Trimming tips = —20°.

Figure 11.— Variation of rudder effectiveness with angle of attack for the $\frac{1}{10}$—scale model of N.R.L. tailless glider tested in Langley free-flight tunnel. Center of gravity = 52—percent center—section chord; q = 3.00 pounds/square foot; design vertical tail; $\delta_c$ = —20°; Trimmers = —20°; Trimming tips = —20°; $\delta_{r_L}$ = 0°.
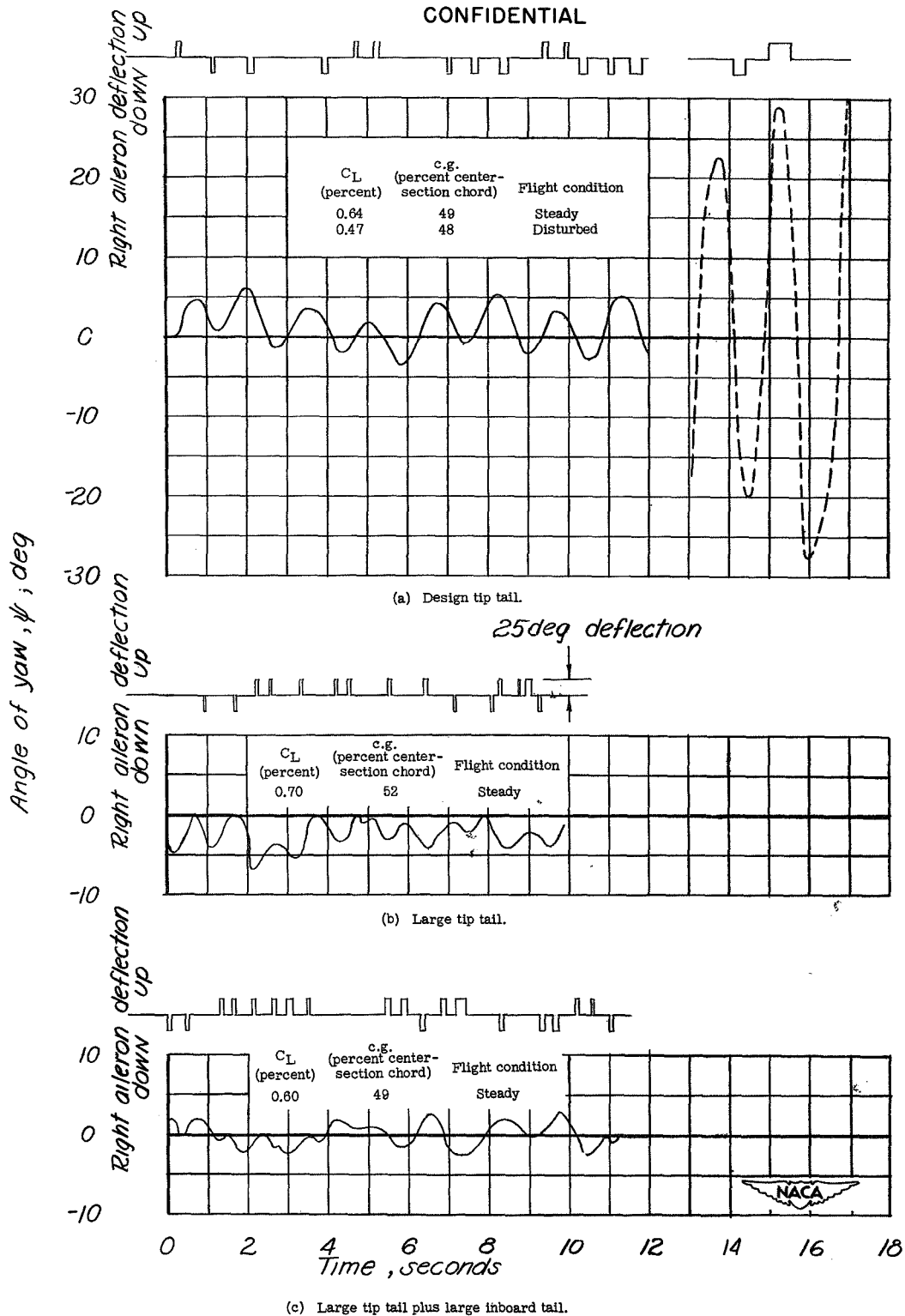
CONFIDENTIAL



(a) Design tip tail.

25deg deflection

(b) Large tip tail.

(c) Large tip tail plus large inboard tail.

Figure 12.— Flight records of $\frac{1}{10}$—scale model of N.R.L. tailless glider obtained in Langley free-flight tunnel. Flap-up configuration; ailerons alone.
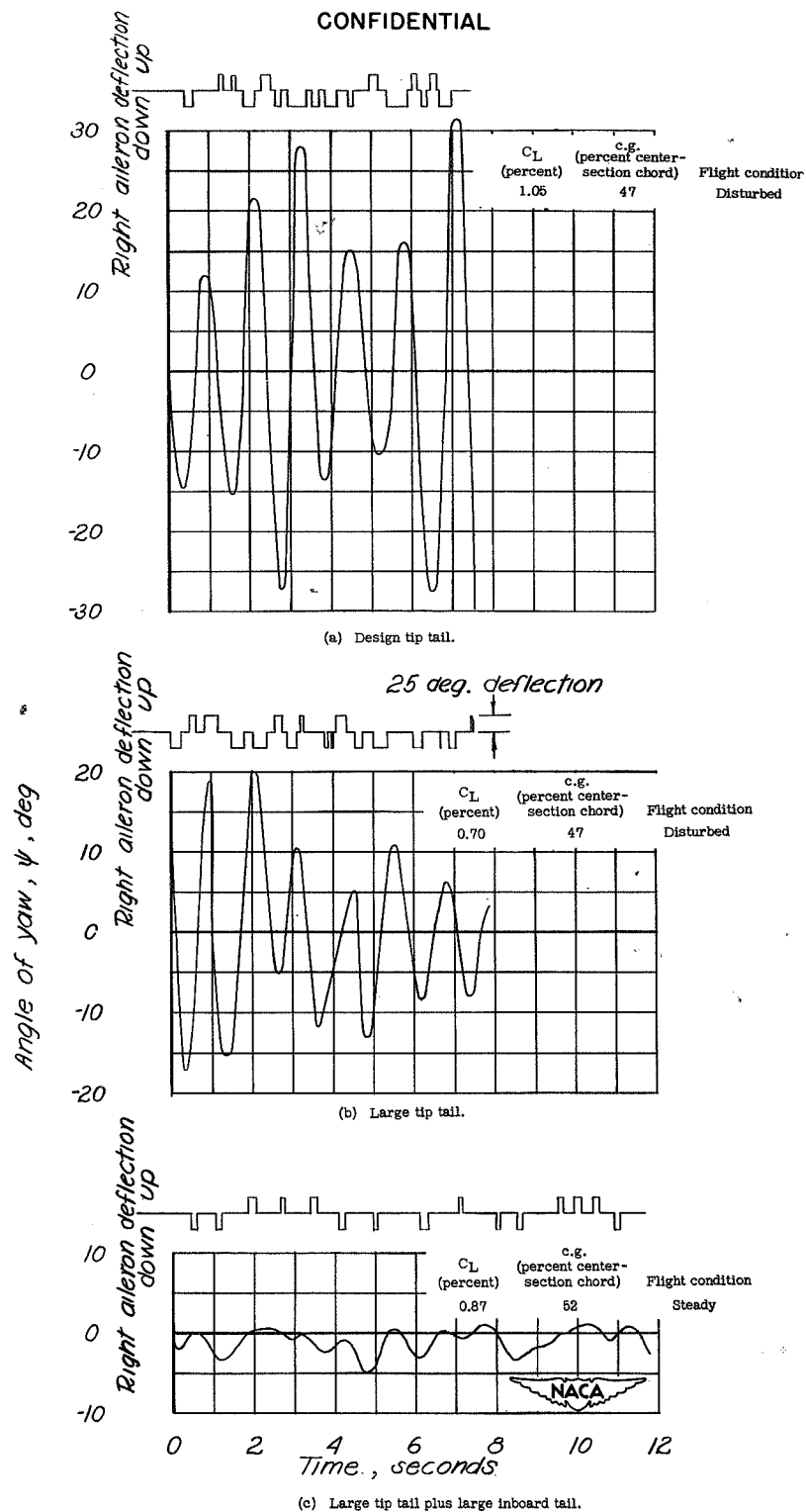
CONFIDENTIAL

Figure 13.— Flight records of $\frac{1}{10}$—scale model of N.R.L. tailless glider obtained in Langley free—flight tunnel. Flap—down configuration; ailerons alone.

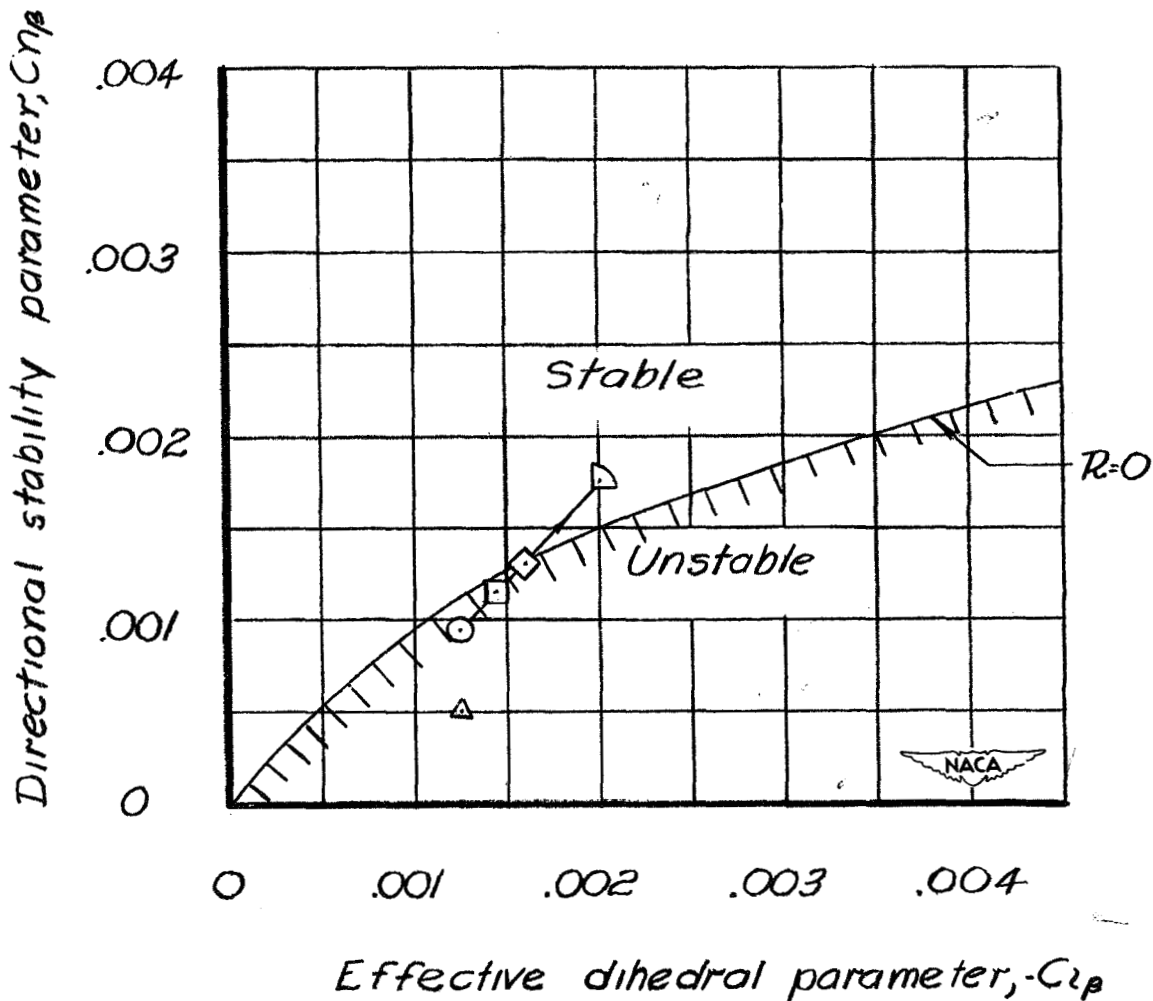| Condition | Source | Configuration |
|:---:|:---|:---|
| ○ | FFT | Design tail |
| □ | FFT | Large tip tail |
| ◇ | FFT | Design tail + large inboard tail |
| ◁ | FFT | Large tip tail + large inboard tail |
| △ | NRCC | Design tail |



Figure 14.— Neutral—lateral—oscillatory—stability boundary for $\frac{1}{10}$—scale model of N.R.L. tailless glider. Flaps up; $C_L = 0.60$.

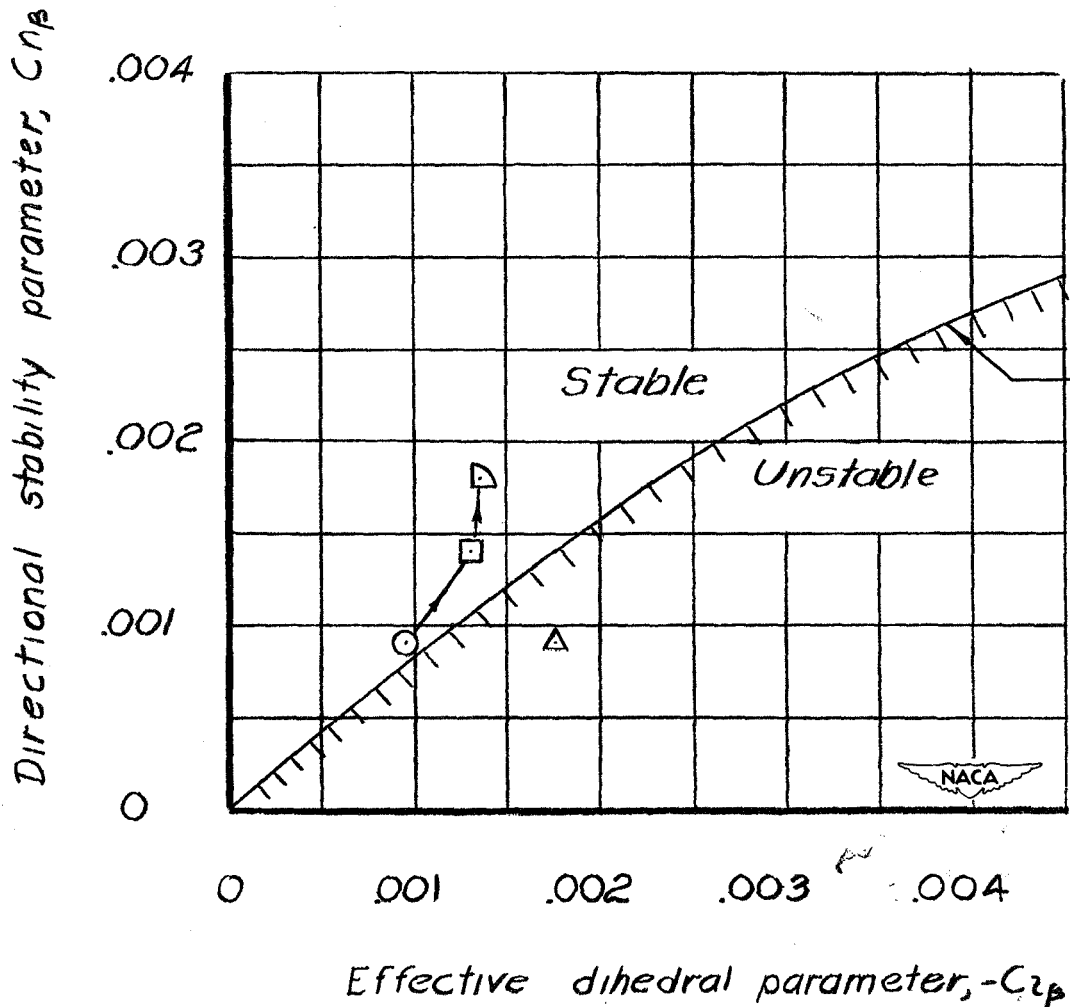| Condition | Source | Configuration |
|-----------|--------|---------------|
| ○ | FFT | Design tail |
| □ | FFT | Large tip tail |
| �৷ | FFT | Large tip tail + large inboard tail |
| △ | NRCC | Design tail |

Figure 15.— Neutral—lateral—oscillatory—stability boundary for $\frac{1}{10}$—scale model of N.R.L. tailless glider.  Flap down; $C_L = 1.2$.

CONFIDENTIAL

| Condition | Tail configuration |
|:---:|:---|
| ○ | Design tip |
| □ | Large tip |
| ◇ | Design tip + large inboard |
| ◁ | Large tip + large inboard |

Time to double amplitude, $T_2$, seconds

Time to damp to one-half amplitude $T_{\frac{1}{2}}$, seconds

Flap up $C_L = 0.60$

Flap down $C_L = 1.2$

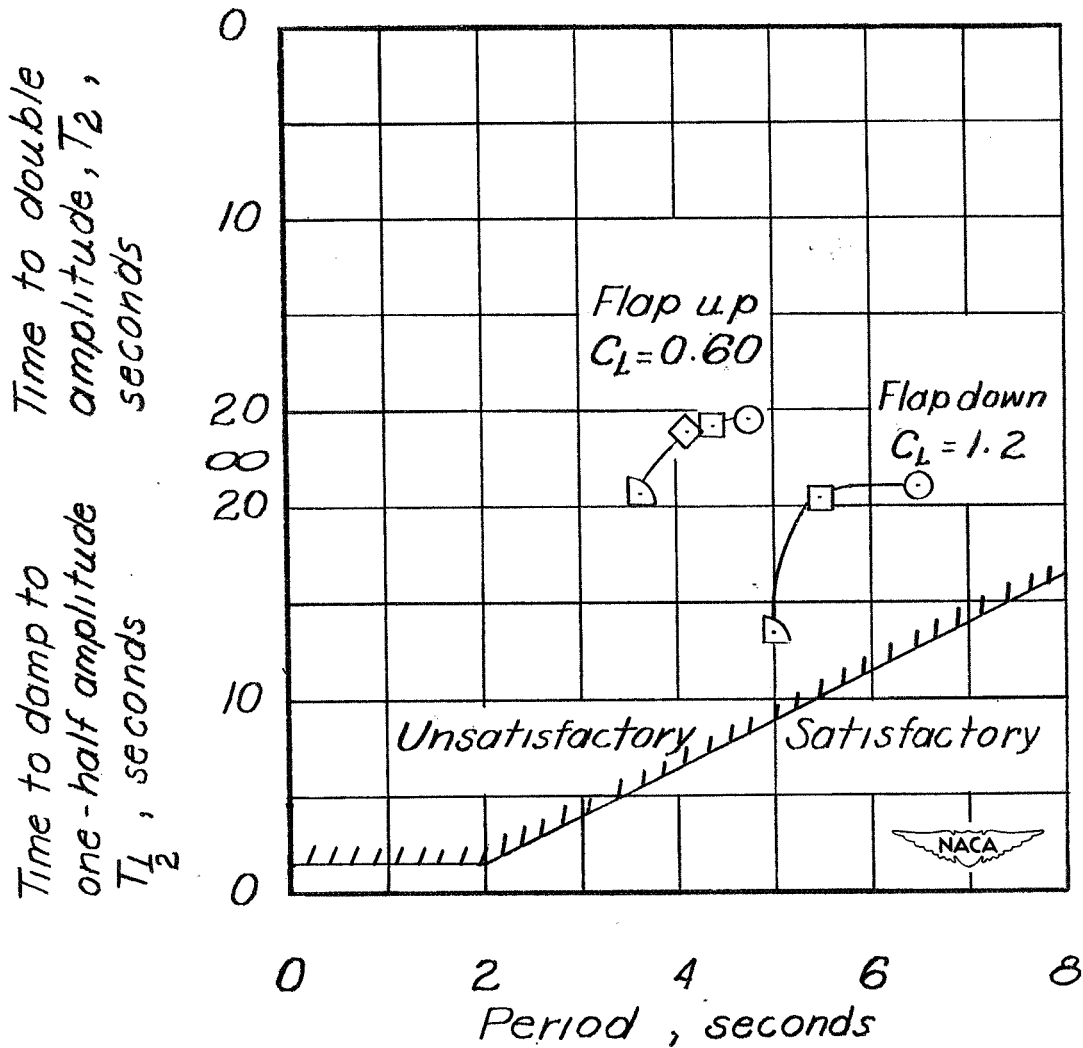Unsatisfactory    Satisfactory

NACA

Period , seconds

Figure 16.— Comparison of calculated damping characteristics of
N.R.L. tailless glider with U. S. Air Force damping specifications.

CONFIDENTIAL